AD-A169 745 AN ANALYTIC THEORY FOR TRAJECTORIES AND CURRENT TO A CYLINDER IN A FLOWING MAGNETOPLASMA(U) AIR FORCE GEOPHYSICS LAB HANSCOM AFB MA C W DUBS ET AL. 1/1

UNCLASSIFIED 22 NOV 85 AFGL-TR-85-0301 F/G 4/1 NL

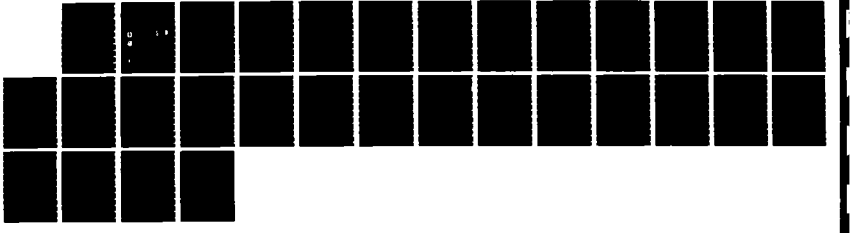

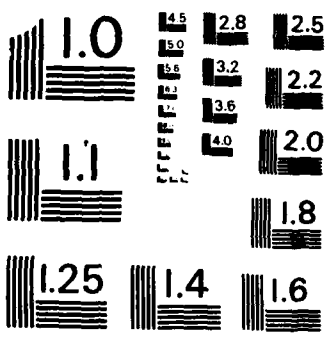

MICROCOPY RESOLUTION TEST CHART

NATIONAL BUREAU OF STANDARDS - 1963 - A

AFGL-TR-85-0301
ENVIRONMENTAL RESEARCH PAPERS, NO. 937

AD-A169 745

An Analytic Theory for Trajectories and Current to a Cylinder in a Flowing Magnetoplasma

CHARLES W. DUBS
MICHAEL HEINEMANN

DTIC
ELECTE
JUL 24 1986
S D
D

22 November 1985

Approved for public release; distribution unlimited.

DTIC FILE COPY

SPACE PHYSICS DIVISION PROJECT 7661
AIR FORCE GEOPHYSICS LABORATORY
HANSCOM AFB, MA 01731

86 7 23 413

"This technical report has been reviewed and is approved for publication"

FOR THE COMMANDER

CHARLES P. PIKE, Chief
Spacecraft Interactions Branch
Space Physics Division

RITA C. SAGALYN, Director
Space Physics Division

This document has been reviewed by the ESD Public Affairs Office (PA) and is releasable to the National Technical Information Service (NTIS).

Qualified requestors may obtain additional copies from the Defense Technical Information Center. All others should apply to the National Technical Information Service.

If your address has changed, or if you wish to be removed from the mailing list, or if the addressee is no longer employed by your organization, please notify AFGL/DAA, Hanscom AFB, MA 01731. This will assist us in maintaining a current mailing list.

Unclassified

SECURITY CLASSIFICATION OF THIS PAGE

A169745

REPORT DOCUMENTATION PAGE

1a. REPORT SECURITY CLASSIFICATION: Unclassified	1b. RESTRICTIVE MARKINGS
2a. SECURITY CLASSIFICATION AUTHORITY	3. DISTRIBUTION/AVAILABILITY OF REPORT: Approved for public release; distribution unlimited
2b. DECLASSIFICATION/DOWNGRADING SCHEDULE	
4. PERFORMING ORGANIZATION REPORT NUMBER(S): AFGL-TR-85-0301 ERP No. 937	5. MONITORING ORGANIZATION REPORT NUMBER(S)
6a. NAME OF PERFORMING ORGANIZATION: Air Force Geophysics Laboratory; 6b. OFFICE SYMBOL (If applicable): PHK	7a. NAME OF MONITORING ORGANIZATION: Air Force Geophysics Laboratory Hanscom AFB, MA 01731
6c. ADDRESS (City, State and ZIP Code): Hanscom AFB Massachusetts 01731	7b. ADDRESS (City, State and ZIP Code)
8a. NAME OF FUNDING/SPONSORING ORGANIZATION; 8b. OFFICE SYMBOL (If applicable)	9. PROCUREMENT INSTRUMENT IDENTIFICATION NUMBER
8c. ADDRESS (City, State and ZIP Code)	10. SOURCE OF FUNDING NOS.

PROGRAM ELEMENT NO.	PROJECT NO.	TASK NO.	WORK UNIT NO.
62101F	7661	11	01

11. TITLE (Include Security Classification): An Analytic Theory for Trajectories (cont)	
12. PERSONAL AUTHOR(S): Dubs, Charles W., and Heinemann, Michael	
13a. TYPE OF REPORT: Scientific Interim; 13b. TIME COVERED: FROM _____ TO _____; 14. DATE OF REPORT (Yr., Mo., Day): 1985 November 22; 15. PAGE COUNT: 28	
16. SUPPLEMENTARY NOTATION	

17. COSATI CODES			18. SUBJECT TERMS (Continue on reverse if necessary and identify by block number)
FIELD	GROUP	SUB GR	
			Flowing magnetoplasma, Electrical potential, Charged particle trajectories, Charging time constant (cont), Space charge current

19. ABSTRACT (Continue on reverse if necessary and identify by block number)

Two-dimensional guiding center theory for a body in a flowing magnetoplasma leads to the electric potential satisfying Laplace's equation outside of (1) the body, (2) one or two forbidden regions, and (3) the inner part of the wake. It is applied to a conducting cylinder larger than the shuttle, of circular cross-section, with radius much less than the length, aligned with the magnetic field, which is perpendicular to the flow vector. Ion and electron trajectories and current to the cylinder are calculated. The effects of collisions, waves, and turbulence are neglected, as is the charge in the forbidden regions and wake. Because of this, the potential and trajectories of the nonimpacting particles are symmetric in the ram and wake. Therefore, the theory results in no particles hitting the wake side and no ion focusing. The steady state potentials result in -0.26 and -0.61 V for cylinder radii of 25 and 250 m, respectively. The result of calculating the charging time constant due to capacitance is the order of 1 ns, which is negligible compared to the transit time. Therefore, the charging time is determined by the transit time (cont)

20. DISTRIBUTION/AVAILABILITY OF ABSTRACT: UNCLASSIFIED/UNLIMITED ☒ SAME AS RPT ☐ DTIC USERS ☐	21. ABSTRACT SECURITY CLASSIFICATION: Unclassified

22a. NAME OF RESPONSIBLE INDIVIDUAL	22b. TELEPHONE NUMBER (Include Area Code)	22c. OFFICE SYMBOL
Charles W. Dubs	617-861-2931	PHK

DD FORM 1473, 83 APR EDITION OF 1 JAN 73 IS OBSOLETE

Unclassified

SECURITY CLASSIFICATION OF THIS PAGE

Block 11 (cont).

and Current to a Cylinder in a Flowing Magnetoplasma

Block 18 (cont).

Analytic theory,
Cylindrical spacecraft,
Two-dimensional theory,
Guiding center,

Block 19 (cont).

and not by capacitance.

ACKNOWLEDGMENTS

We are grateful to David Cooke for stimulating discussions and to Maurice Tautz for calculations with the POLAR code.

Accesion For
NTIS CRA&I ☑
DTIC TAB ☐
Unannounced ☐
Justification .....
By .....
Distribution /
Availability Codes
Dist | Avail and / or Special
A-1

QUALITY INSPECTED 4

Contents

Illustrations

Illustrations

Tables

An Analytic Theory for Trajectories and Current to a Cylinder in a Flowing Magnetoplasma

1. INTRODUCTION

Accurate comprehensive equations for the electrical behavior of spacecraft and plasma in the vicinity cannot be solved analytically. Therefore, either they have been solved numerically with time consuming computer programs, or many simplifying assumptions have been made.

The theory of electric probes with simple geometry in a stationary plasma with or without a magnetic field has been treated fairly fully.[1,2,3,4,5,6] Much

(Received for publication 30 October 1985)

1. Kagan, Y.M., and Perel, V.I. (1964) Probe methods in plasma research, Sov. Phys.-Usp. 81:767-793.

2. Chen, F.F. (1965) Electric probes, in Plasma Diagnostic Techniques, R.H. Huddlestone and S.L. Leonard, Eds., Academic Press, New York, 113-200.

3. Laframboise, J.G. (1966) Theory of Spherical and Cylindrical Langmuir Probes in a Collisionless, Maxwellian Plasma at Rest, U.T.I.A.S. Report 100.

4. Chung, P.M., Talbot, L., and Touryan, K.J. (1974) Electric probes in stationary flowing plasmas: Part 1. Collisionless and transitional probes, AIAA J. 12:133-154.

5. Sanmartin, J.R. (1970) Theory of a probe in a strong magnetic field, Phys. Fluids, 13:103-116.

6. Rubinstein, J., and Laframboise, J.G. (1983) Aligned spheroids, finite cylinders, and disks, Phys. Fluids 26:3624-3627.

work has also been done on probes in flowing plasmas.[7,8,9,10,11] Less work has been done on the more complicated problem of a probe in a flowing magnetoplasma. Rough calculations of the effect of magnetic field $\vec{B}$ on satellite drag were made by Brundin[12] and Drell et al.[13] Whipple[14] showed that, as the gyroradius decreases from 100 to 0.01 of the sphere radius, the current to a sphere decreases to one-half. By numerical solution of Vlasov's and Poisson's equations, Grabowski and Fischer[15] and Brooks and Koehler[16] obtained the ion density dependence on radius and azimuth of a cylinder parallel to the magnetic field moving perpendicular to it. Grabowski and Fischer found that, for equal spacecraft and ion thermal speeds, the magnetic field became quite important when the gyroradius decreased to the cylinder radius. They did not consider the case of smaller gyroradii. Brooks and Koehler considered sounding rockets with radius smaller than the ion gyroradius and so neglected magnetic field effects.

In this paper, simplifying assumptions are made and a new method explored that permits an analytical solution of the electrical characteristics. Application to low equatorial Earth satellites larger than the shuttle is envisioned. The basic theory is presented in the next section. It is then applied to a cylinder parallel to the magnetic field.

---

7. Call, S.M. (1969) The interaction of a satellite with the ionosphere, School Eng. Appl. Sci., Columbia U. Plasma Lab. Rept. No. 46.

8. Gurevich, A.V., Pitaevskii, L.P., and Smirnova, V.V. (1969) Ionospheric aerodynamics, Space Sci. Rev. 9:805-871 or (1970) Sov. Phys.-Usp. 99:595-616.

9. Al'pert, J.J. (1976) Wave-like phenomena in the near-earth plasma and interactions with man-made bodies, in Handbuch der Phys., Geophys III, K. Rawer, Ed., pp. 217-349.

10. Whipple, E.C. (1981) Potentials of surfaces in space, Reprints Progr. Phys. 44:1197-1250.

11. Garrett, H.B. (1981) The charging of spacecraft surfaces, Rev. Geophys. Space Phys. 19:577-616.

12. Brundin, C.L. (1963) Effects of charged particles on the motion of an Earth satellite, AIAA J. 11:2529-2538.

13. Drell, S.D., Foley, H.M., and Ruderman, M.A. (1965) Drag and propulsion of large satellites in the ionosphere; an Alfven propulsion engine in space, Phys. Rev. Lett. 14:171-175.

14. Whipple, E.C. (1965) The Equilibrium Electric Potential of a Body in the Upper Atmosphere and in Interplanetary Space. Ph.D. thesis, George Washington U., Washington, D.C.

15. Grabowski, B., and Fischer, T. (1975) Theoretical density distribution of plasma streaming around a cylinder, Planet. Space Sci. 23:287-304.

16. Brooks, W.S.C., and Koehler, J.A. (1980) The ram effect for a conducting cylinder in a drifting plasma, Can. J. Phys. 58:224-231.

2. BASIC THEORY

This paper concerns the case of a conducting body moving perpendicular to a known uniform magnetic field with constant velocity $\vec{V}_o$ in a magnetoplasma. The formalism for describing the motion of the plasma particles is the guiding center approximation. This is valid when the gyroradius times each component of electric field gradient is much smaller than the electric field. Except where the electric field nearly vanishes, this holds when the gyroradius is small compared to the body dimensions. The effect of the finite size of the gyroradius is neglected. As in Northrup,[17] the lowest ("zeroth") and next ("first," m/e times zeroth) order terms are kept, and particle motion is averaged over a gyroperiod. Steady laminar flow is assumed, and plasma oscillations are neglected. Boltzmann's equation is not used. The ion thermal speed is smaller than the ion drift speed and, for simplicity, is neglected. The treatment is two-dimensional, and thus, for example, is applicable to the magnetic field parallel to a cylinder of length large compared to other dimensions. The ambient plasma is assumed to be uniform, collisionless, and without electric field. The magnetic and the electric fields are assumed to be time independent in the frame of the body, the frame in which the calculation is made. Therefore, the electric field, $\vec{E} = -\nabla\Phi$.

Only nonrelativistic velocities are considered; the magnetic field caused by currents is negligible and so is neglected. All charges reaching the body are assumed to be absorbed; no scattering, photo, or secondary emission is assumed. The latter assumption is valid for the low particle energies considered here. For simplicity, the force of gravity is neglected since it is relatively small. In MKS units with the z-axis chosen in the direction of the magnetic field $\vec{B}$, the drift velocity of the center of gyration of a particle is given by Eq. (1.17) of Northrop[17] as

$$\vec{V}_\perp = \frac{\vec{B}}{B^2} \times \left[-\vec{E} + \frac{M}{e} \nabla B + \frac{m}{e} \left(-\vec{g} + v_\parallel \frac{d\hat{z}}{dt} + \frac{d\vec{V}_E}{dt} \right) \right]. \tag{1}$$

M, m, e, and $v_\parallel$ are the particle's magnetic moment, mass, charge (including sign), and component of velocity parallel to $\vec{B}$ respectively; $\vec{g}$ is the acceleration of gravity.

---

17. Northrop, T.G. (1963) The Adiabatic Motion of Charged Particles, Interscience Publishers, p. 8.

$$\vec{V}_E \equiv \frac{\vec{E} \times \vec{B}}{B^2} \tag{2}$$

is the zeroth order drift velocity. From the assumptions above, the second, third, and fourth (middle) terms of the right-hand side of Eq. (1) are neglected and $\vec{V} = \vec{V}_\perp$. Since $\vec{B}$ is constant and $\partial/\partial t = 0$, the last term becomes $m/(eB^2)\vec{V} \cdot \nabla \vec{E}$. So (to the first order), Eq. (1) becomes

$$\vec{V} = \vec{V}_E + \vec{V}_1, \tag{3}$$

where

$$\vec{V}_1 \equiv \frac{m}{eB^2} \vec{V}_E \cdot \nabla \vec{E}. \tag{4}$$

The latter is the first order drift velocity, often called the "polarization" drift. At the surface of the conductor, $\vec{E}$ is perpendicular to the conductor, so $\vec{V}_E$ is tangential to the conductor. Therefore, to zeroth order, the charged particles go around the conductor without hitting it. The total guiding center energy, ε, of a particle is a constant of motion. Since, to first order,

$$\varepsilon = \frac{m}{2} V_E^2 + e\phi, \tag{5}$$

this is constant along the guiding center trajectory, that is, along a streamline of the specie. For this two-dimensional case,

$$\vec{V} = \frac{1}{eB^2} \frac{\vec{B} \times \nabla \varepsilon}{1 - \frac{m}{eB^2} \nabla \cdot \vec{E}} \tag{6}$$

is consistent with Eq. (3). This may be seen by writing out the four terms in Eq. (4) from the components of the vectors, substituting $1 + m/(eB^2)\nabla \cdot \vec{E}$ for $[1 - m/(eB^2)\nabla \cdot \vec{E}]^{-1}$ in Eq. (6), using Eq. (2) in Eq. (5), which is then substituted into Eq. (6), and writing out the terms. From Eqs. (3), (4), and (6), the current density of specie α is

$$\vec{J}_\alpha = n_\alpha e_\alpha \vec{V}_\alpha \quad n_\alpha e_\alpha \vec{V}_E + \frac{\rho_\alpha}{B^2} (\vec{V}_E \cdot \nabla)\vec{E} \tag{7}$$

$$= N_\alpha \frac{\vec{B}}{B^2} \times \nabla \varepsilon_\alpha, \tag{8}$$

where n_α is the number density,

$$N_\alpha \equiv \frac{n_\alpha}{1 - \frac{m_\alpha}{e_\alpha B^2} \nabla \cdot E}, \tag{9}$$

and the mass density is

$$\rho_\alpha \equiv m_\alpha n_\alpha. \tag{10}$$

Taking the divergence of Eq. (8) and using vector identities,

$$e_\alpha \nabla \cdot (n_\alpha \vec{V}_\alpha) = \frac{\vec{B}}{B^2} \cdot (\nabla \varepsilon_\alpha \times \nabla N_\alpha). \tag{11}$$

From charge conservation (the continuity equation), Eq. (11) = 0. From this, N_α can be proven to equal $N_\alpha(\varepsilon_\alpha)$, that is, to depend on coordinates only through its dependence on ε_α. Thus, it is a constant along a streamline. Since $N_\alpha = n_\alpha$ at ∞, it is independent of ε_α and is the same (a constant) everywhere that the streamline goes, that is, everywhere except in forbidden regions and the part of the wake that is free from these streamlines because of sweptout impacting particles. Writing Eq. (9) as $N_\alpha = n_\alpha[1 + (m_\alpha / e_\alpha B^2)\eta/\epsilon_o]$ from expansion and Poisson's equation, multiplying it by e_α and summing over α,

$$\sum_\alpha e_\alpha N_\alpha = \eta \left(1 + \frac{\rho}{\epsilon_o B^2}\right), \tag{12}$$

where $\eta \equiv \sum_\alpha e_\alpha n_\alpha$ and $\rho \equiv \sum_\alpha \rho_\alpha$. Since (1) the left side of Eq. (12) is the same everywhere except in the regions in which streamlines of one or more species are missing, (2) it vanishes at ∞ and thus also in this region, and (3) the parenthesis on the right-hand side is always positive, then η must vanish throughout this region. Therefore, $\nabla \cdot \vec{E} = 0$ from Poisson's equation, and $N_\alpha = n_\alpha$ from Eq. (9).

The current to the surface of the body is

$$I = -\sum_\alpha \int J_{\alpha n} dA, \tag{13}$$

where

$$J_{\alpha n} = \frac{\vec{E}}{E} \cdot \vec{J}_\alpha = \frac{\rho_\alpha}{B^3}\left[\left(\frac{\vec{E}}{E} \times \hat{z}\right) \cdot \nabla\right]\frac{E^2}{2} \tag{14}$$

from Eqs. (2) and (7). A is the surface area of the body, and $\vec{E}$ is the electric field at the surface. $J_{\alpha n}$ is seen to be independent of e_α and to come only from the polarization drift (first order, no zeroth order part). Thus, the charging current, I, also is only a first order current. Let $\vec{y}$ be the distance vector from the center of the spacecraft in the $\vec{B} \times \vec{V}_o$ direction. If, for each specie α, all and only particles upstream having $y_{\alpha m} < y_\alpha < y_{\alpha M}$ at ∞ hit the body, then it may be simpler to obtain the current per unit length from

$$I_L = a\sum_\alpha J_{\alpha\infty}(y_{\alpha M} - y_{\alpha m}), \tag{15}$$

where $J_{\alpha\infty}$ is the current density far upstream.

3. APPLICATION

The theory is applied to a right, circular, conducting cylinder of radius a and half length ba. (All lengths except a and R_g are normalized to a.) The origin of the coordinate system is taken at the center of the cylinder, the x-axis in the direction of the flow velocity, $-\vec{V}_o$, in the cylinder frame, and the z-axis in the $\vec{B}$ and cylinder axis direction (Figure 1). First, the potential, ϕ, then the energy per particle, $\mathcal{E}$, are calculated in the cylinder frame. The potential resulting from nonzero charge density in the sheath, the forbidden region (see below), and in the part of the wake with missing streamlines resulting from ram sweepout is neglected, although it must be significant. The potential is

$$\phi = \phi_p + \phi_q, \tag{16}$$

where ϕ_p is that due to the electric field from the motion and the polarization charge on the cylinder caused by this field, and ϕ_q is the potential caused by a net charge q on the cylinder. ϕ_p is the solution of Laplace's equation with z = 0 for the cylinder with no net charge in a background electric field $V_oB\hat{y}$:

$$\phi_p = -V_oBRaf \sin \phi, \tag{17}$$

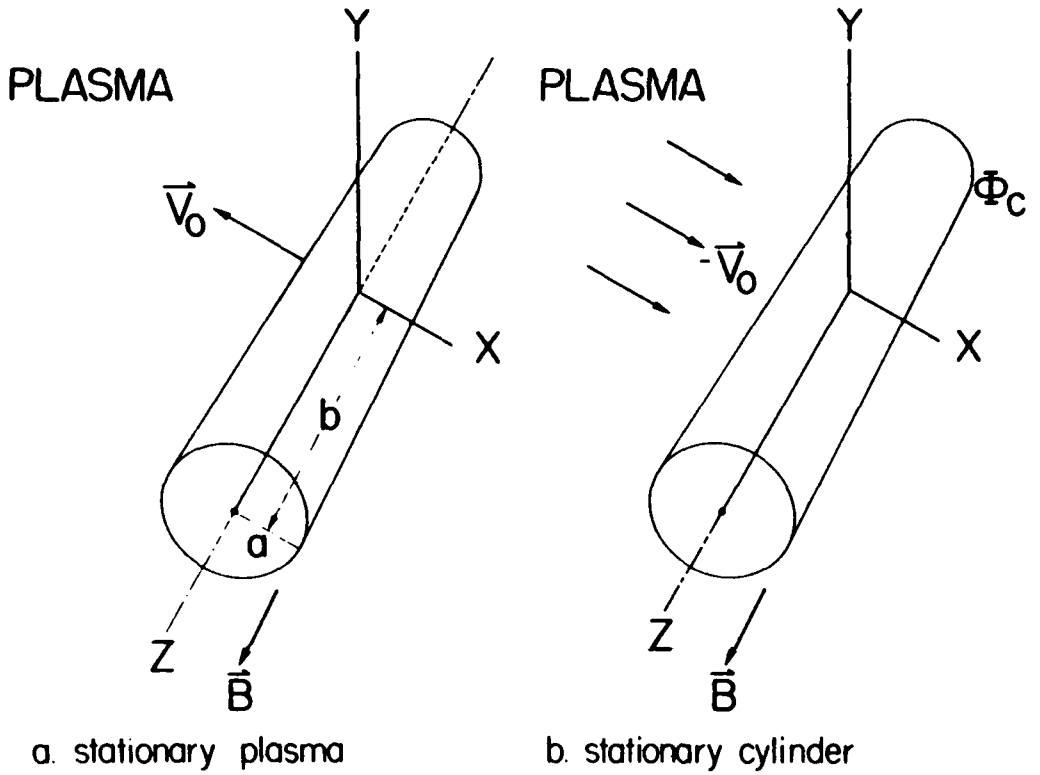

Figure 1. Relative Motion Between Cylinder and Magnetoplasma: Two Frames of Reference

where $\phi \equiv \angle x, R$. For $R << b$, $f = 1 - 1/R^2$; for $R >> b$, $f = 1 - b/R^3$. For all ranges of R, f is taken as $p - b/[R^2(b + R)]$, where $p \equiv b/(b + 1)$ (to make ϕ_p vanish for R = 1). An empirical formula[18] for z = 0 is used for ϕ_q,

$$\phi_q = \frac{cgq}{a}\left[\left(1 + \frac{b}{R}\right)^u - 1\right], \tag{18}$$

where $g = 1/(4\pi\epsilon_o)$, c = 1.777, and u = 1/(cb). So the potential is taken as

18. Dubs, C. W. (1982) Potentials and Charges on Conducting Rocket Sections, AFGL-TR-82-0349, AD A130143, p. 29, Eq. (A11).

$$\Phi = -V_o BRa\left[p - \frac{b}{R^2(b+R)}\right]\sin\phi + K\Phi_c\left[\left(1+\frac{b}{R}\right)^u - 1\right], \tag{19}$$

where

$$\Phi_c = \frac{cgq}{Ka}, \tag{20}$$

the potential of the cylinder, and

$$K \equiv \left[(b+1)^u - 1\right]^{-1}. \tag{21}$$

Figure 2 shows a cross section of equipotential surfaces in the cylinder frame for a set of parameters with $b >> 1$ and $\Phi_c = 0$. Outside of the cylinder, $\Phi < 0$ for $y > 0$, and $\Phi \geq 0$ for $y < 0$.

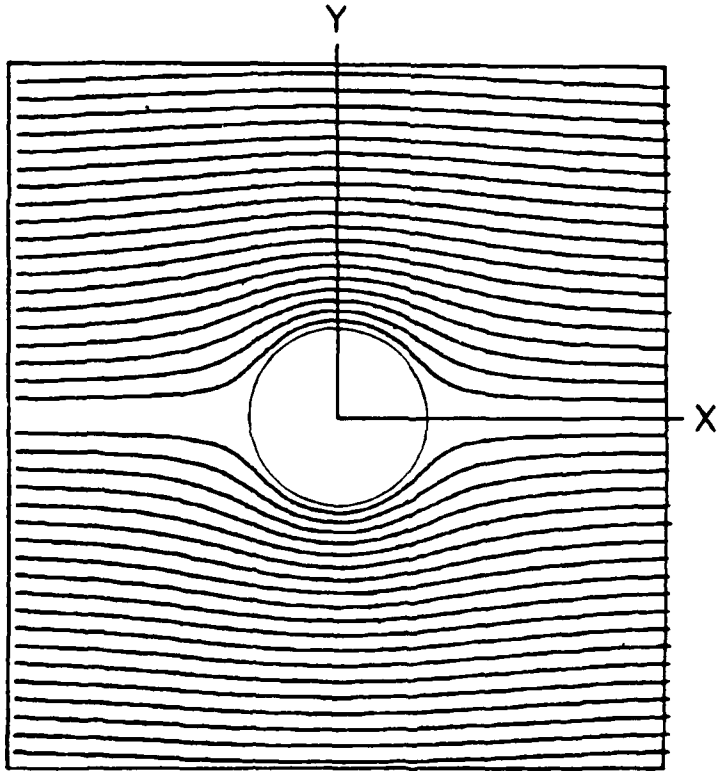

Figure 2. Equipotential Surfaces for $\Phi_c = 0$. $\Phi = 0$ on the plane with the missing contour

Figure 3 is the same, except that $\phi_c > 0$. $\phi < 0$ for y greater than the value on the missing contour, and $\phi > 0$ for y smaller. Because of the small mass of electrons, $V_1 << V_E$, so ambient electrons nearly follow the equipotential curves.

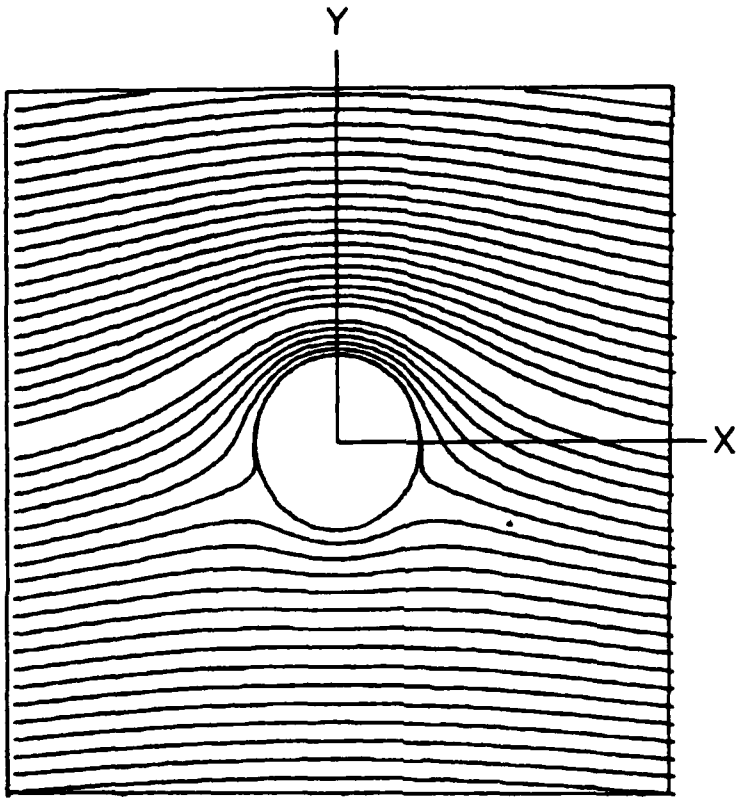

Figure 3. Equipotential Surfaces for $\phi_c > 0$. $\phi = 0$ on the open cylindrical surface with the missing contour

From Eqs. (2) and (5),

$$\frac{\varepsilon}{e} = \frac{m(E_R^2 + E_\phi^2)}{2eB^2} + \phi. \tag{22}$$

Since ε is the same if ϕ be replaced with $\pi - \phi$, it and the trajectories that miss the cylinder are symmetric in x. This means that the charge distribution in the wake is the mirror image of that in the ram (the x and y components of velocity at

symmetric points are the same except for the sign of the y component) except that the wake is missing the particles that hit the cylinder. Ion focusing in the wake is not obtained because of omitting the potential of the electrons in the forbidden region and wake. For V_o = 8 km/sec, y = 0, and R = ∞, ε/e is 0.00018V for electrons and 5.3 V for O^+ ions. The gyroradius of electrons is 2 cm and that of O^+ ions 4 m when moving perpendicular to a 0.5 G magnetic field with 0.1 eV energy. For an orbiting cylinder with a = 2.5 m and ba = 10 m (the approximate size of a shuttle), the theory would hold for electrons but not for O^+ ions. So, application is made to a cylinder ten or a hundred times larger. (Earth satellites this large are anticipated within a few decades.)

Trajectories of the guiding center are obtained as follows: Eq. (19) and $\vec{E} = -\nabla\phi$ are used in Eq. (22), $\sin\phi$ is set equal to y/R, and the result is equated to the limit of the same expression as $R \to \infty$. This gives

$$\frac{2\varepsilon}{mV_o^2} = p(p - c_1 y_\infty) = \left\{\left[p + \frac{b(b+2R)}{R^2(b+R)^2}\right]\frac{y}{R} + \frac{c_2}{R^2\,(1+b/R)^{1-u}}\right\}^2$$

$$+ \left(1 - \frac{y^2}{R^2}\right)\left[p - \frac{b}{R^2(b+R)}\right]^2$$

$$- c_1\left[p - \frac{b}{R^2(b+R)}\right]y + cc_1c_2\left[\left(1+\frac{b}{R}\right)^u - 1\right], \qquad (23)$$

where y_∞ is the limit of y as $R \to \infty$, that is, the impact parameter;

$$c_1 \equiv \frac{2a}{R_g} \equiv \frac{2eBa}{mV_o}, \qquad (24)$$

and

$$c_2 \equiv \frac{K\phi_c}{caV_oB}. \qquad (25)$$

Eq. (23) may be written as

$$Dy^2 + Fy + G = 0, \qquad (26)$$

where D, F, and G are functions of R and are independent of y. The solution for y and

$$x = t\sqrt{R^2 - y^2} \tag{27}$$

give the trajectory parametric in R. The "+" sign in Eq. (27) has physical meaning only for trajectories that do not hit the cylinder. For ϕ_c not too negative for electrons and not too large for positive ions, minimum and maximum values, $y_{\infty m}$ and $y_{\infty M}$, of y_∞ exist such that trajectories starting at large -x for which $y_{\infty m} < y_\infty < y_{\infty M}$ hit the cylinder. Trajectories with $y_\infty < y_{\infty m}$ pass the cylinder with $y_\infty < -1$ (at x = 0), and those with $y_\infty > y_{\infty M}$ pass the cylinder with $y_\infty > 1$. Figure 4 shows the two O^+ trajectories for the parameter values in Table 1, a = 25 m, and $y_\infty = y_{\infty m}$ and $y_{\infty M}$. For -x starting large and $y_{\infty m} < y_\infty < y_{\infty M}$, x < 0 for all parts of the trajectory. Analytical means of obtaining $y_{\infty m}$ or $y_{\infty M}$ are not feasible for these types of trajectories. They may be obtained to any desired accuracy, however, as follows: From Eqs. (23) to (26), set $F^2 - 4DG = 0$, solve for y_∞, and obtain its minimum value as R is varied. This gives $y_{\infty M}$. The value of $y_{\infty m}$ is obtained by solving Eq. (23) for y_∞, setting y = -R, and finding the maximum value of y_∞ as R is varied. Mathematically, bounded ion trajectories exist in the forbidden regions, the shaded ones in Figures 4 through 6. Since no ion emission is assumed, no ions should exist there, so they are ignored here. The sign of $\sqrt{F^2 - 4DG}$ in the solution for y depends on whether a bounded or unbounded trajectory is being considered or, if an unbounded, whether R is increasing or decreasing.

Table 1. Values of Parameters Used Not Specified Otherwise

parameter	value	parameter	value
c	1.777	B	0.5 G
V_o	7 km/sec	ϕ_c	-0.5 V
a	25 or	n	10^{11} m^{-3}
	250 m	T	2000° K
b	4		

Figure 5 shows the same as Figure 4 except that $\phi_c = \phi_{cM}$, the maximum value for any ions to hit the cylinder. For this case, $y_{\infty m} = y_{\infty M}$.

Figure 6 shows the same as Figure 4 except that the cylinder is ten times larger. The limiting trajectories are seen to be different, simpler types. For

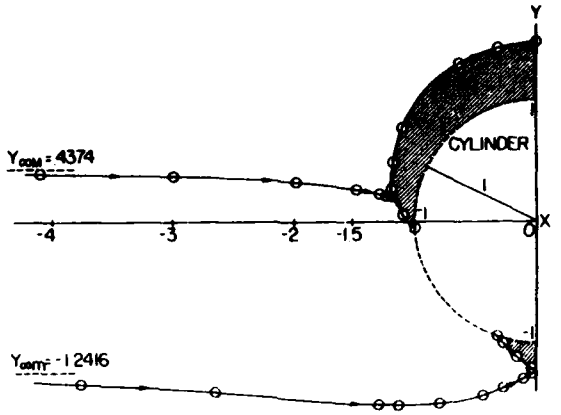

Figure 4. Limiting O^+ Trajectories for B = 0.5 G, V_o = 7 km/sec, ϕ_c = -0.5 V, b = 4, and a = 25 m

them, $y_{\infty m}$ and $y_{\infty M}$ may be obtained from the maximum and minimum values of the solution of Eq. (23) for y_∞ with $R = 1$ and $-1 \leq y_{1m} \leq y_{1M} \leq 1$. For $y_\infty = y_{\infty m}$ and this set of parameters (ϕ_c = -0.5 V) but varying a, the transition between the two types of trajectories in Figures 4 and 6 occurs at a = 46.6 m. This is determined by differentiating Eq. (23) with respect to R, equating it and dy/dR to zero, setting R = 1, and solving (a cubic equation) for a. The maximum ya of the forbidden region is seen to be 0.5 or $0.8 R_g$ [see Eq. (24)] from the cylinder for a = 25 or 250 m, respectively.

For the simple type of trajectories in Figure 6, the difference of the two limiting values of y_∞ is

$$y_{\infty M} - y_{\infty m} = \frac{b}{(b+1)\,|c_1|}\left[\frac{(b+1)^u c_2}{b} - \frac{e}{|e|}\,\frac{2b+3}{b+1}\right]^2 . \qquad (28)$$

This holds when the bracket is not positive for $e > 0$ and not negative for $e < 0$. From this and Eq. (25), as expected, it is seen that this difference increases for electrons and decreases for ions as ϕ_c increases. ϕ_{cM} is the value of ϕ_c for which the bracket in Eq. (28) vanishes. $y_{\infty M} - y_{\infty m}$ is zero for $\phi_c/\phi_{cM} \doteq 1$. For the previously used parameters, ϕ_{cM} = 27.7 V for a = 25 m and ϕ_{cM} = 277 V

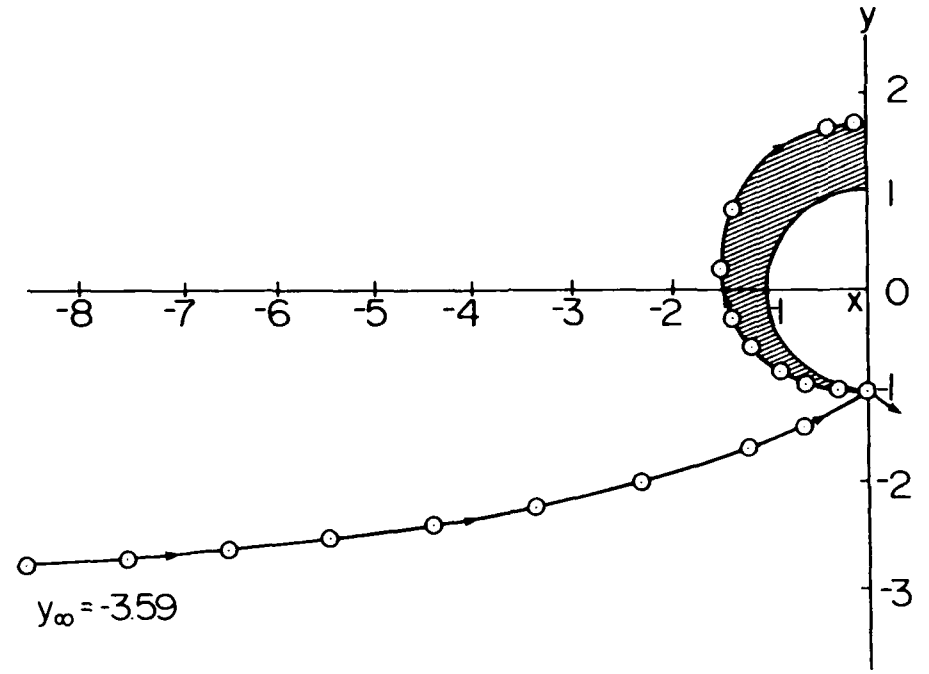

Figure 5. Limiting O^+ Trajectories for B = 0.5 G, V_O = 7 km/sec, Φ_c = Φ_{cM} = 27.7 V, b = 4, and a = 25 m

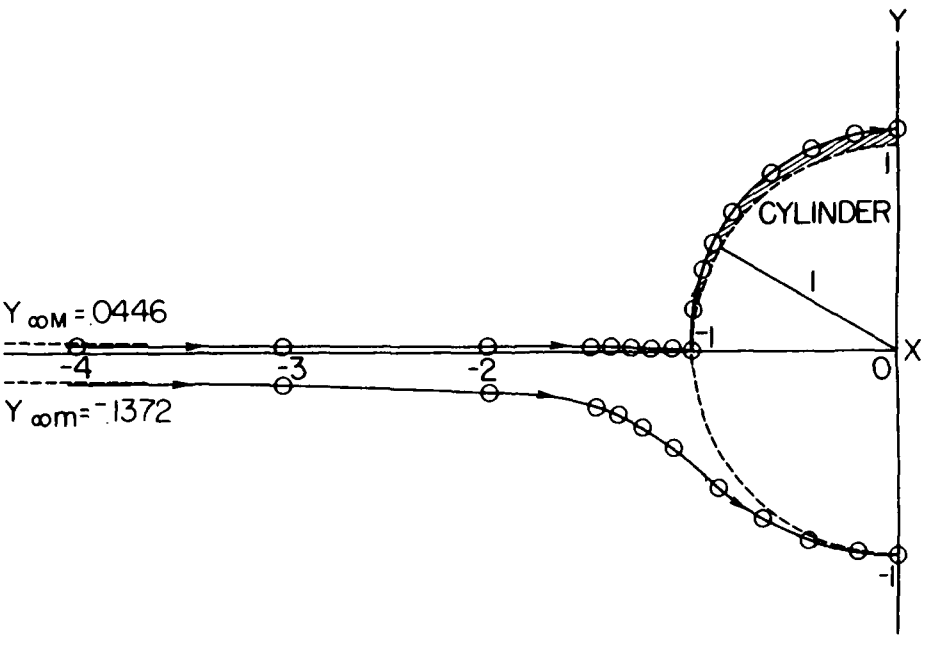

Figure 6. Limiting O^+ Trajectories for B = 0.5 G, V_O = 7 km/sec, Φ_c = - 0.5 V, b = 4, and a = 250 m

for a = 250 m. For ions and $\Phi_c > \Phi_{cM}$, the value of y_∞ which divides the trajectories passing the cylinder with $y > 1$ from those with $y < -1$ is determined as described above for obtaining the value of $y_{\infty m}$. Table 2 shows some values of $y_{\infty m}$, $y_{\infty M}$, and their difference, along with those of y_{1m} and y_{1M}, the corresponding limiting values of y where the particle hits the cylinder. The results for b = 4 are seen to be close to those for $b = \infty$. As $b \to \infty$, the term containing c_2 in Eq. (28) vanishes, so, although the trajectories are affected by Φ_c, $y_{\infty M} - y_{\infty m}$ and thus the current per unit length to the side are independent of it. The values of $y_{\infty M} - y_{\infty m}$ for O^+ and $\Phi_c \leq 0$ are seen generally to be much less than 2, the minimum value without magnetic field. This indicates that the magnetic field decreases the particle currents to the cylinder and the y extent of the wake.

For simplicity, the current to the cylinder is determined assuming only current from ambient electrons, I^-, and O^+ ions, I^+. The current due to each specie is the sum of I_s, the current to the sides (curved surface), and I_e, that to the ends. The steady state potential is the value making the net current zero. The current to the sides is given by Eq. (15). For each specie,

$$I_s = neV_o\, 2ba^2\, (y_{\infty M} - y_{\infty m}). \tag{29}$$

This gives the ram current without magnetic field and $\Phi_c = 0$ if $y_{\infty M} - y_{\infty m} = 2$. I_s^+ vs Φ_c for the parameter values in Table 1 with a = 250 m is shown in Figure 7. Its shape is parabolic since, from Eq. (25), Eq. (28) and thus I_s^+ are quadratic functions of Φ_c, at least for the simple type of trajectories. For electrons, b = 4 and a = 250 m: I_s^- is $\sim 10^{-4}$ of I_e^- and thus is omitted. Since the thermal speed, Eq. (32), for electrons is ten times V_o, the electron current may be calculated neglecting the cylinder's motion. Since the electron gyroradius $r_g \sim 2$ cm so that $a/r_g \sim 12{,}500$, according to Rubinstein and Laframboise[6] (consistent with the top six numbers in the last column of Table 2), the electron current to the sides is negligible, and the currents to the ends are

$$I_e^+ = ne_+ v_{T+} 2\pi a^2, \tag{30}$$

and, for $\Phi_c < 0$,

$$I_e^- = ne_- v_{T-} 2\pi a^2 \exp\left[-e_- \Phi_c/(kT_-)\right], \tag{31}$$

where k is Boltzmann's constant and

Table 2. Minimum and Maximum Particle Impact y Coordinates and Impact Parameters in Cylinder Radii

col. 1		2	3	4	5	6	7	8	9	10	11
quantity		a	b	ϕ_c	c_1	c_2	y_{1m}	y_{1M}	$y_{\infty m}$	$y_{\infty M}$	$y_{\infty M}-y_{\infty m}$
row	specie	m		V							
1	e^-	2.5	∞	0	-6.28 +3	0	0	1	-1.59 -4	4.78 -4	6.37 -4
2	e^-	2.5	4	0	-6.28 +3	0	0	1	-1.27 -4	4.89 -4	6.16 -4
3	e^-	2.5	4	.0845	-6.28 +3	.214	- .0305	1	- .121	- .120	6.55 -4
4	e^-	250	4	- .5	-6.28 +5	- .0127	1.80 -3	1	7.14 -3	7.15 -3	6.14 -6
5	e^-	250	4	0	-6.28 +5	0	0	1	-1.27 -6	4.89 -6	6.16 -6
6	e^-	250	4	8.45	-6.28 +5	.214	- .0305	1	- .121	- .121	6.55 -6
7	O^+	25	4	- .5	2.14	- .127	- .947	- .0525	-1.24	.437	1.68
8	O^+	25	4	- .2	2.14	- .0506			-1.26	.394	1.65
9	O^+	25	4	27.7	2.14	7.02	-1	-1	-3.59	-3.59	0
10	O^+	250	4	-40	21.4	-1.01	-1	.144	.372	.609	.237
11	O^+	250	4	-20	21.4	- .506	-1	.0721	.115	.323	.208
12	O^+	250	4	-10	21.4	- .253	-1	.0361	- 0141	.180	.194
13	O^+	250	4	- 5	21.4	- .127	-1	.0180	- .0788	.109	.188
14	O^+	250	4	- 2	21.4	- .0506	-1	7.21 -3	- .118	.0660	.184
15	O^+	250	4	- 1	21.4	- .0253	-1	3.61 -3	- .131	.0517	.182
16	O^+	250	∞	- .5	21.4	- ∞	-1	0	- .135	.0525	.187
17	O^+	250	4	- .5	21.4	- .0127	-1	1.80 -3	- .137	.0446	.182
18	O^+	250	∞	0	21.4	indef.	-1	0	- .140	.0468	.187
19	O^+	250	4	0	21.4	0	-1	0	- .144	.0374	.181
20	O^+	250	4	8.45	21.4	.214	-1	- .0305	- .253	- .0833	.170
21	O^+	250	4	98.8	21.4	2.5	-1	- .356	-1.45	-1.37	.0750
22	O^+	250	4	198	21.4	5.	-1.	- .713	-2.80	-2.78	.0150
23	O^+	250	4	230	21.4	5.82	-1	- .830	-3.25	-3.25	5.26 -3
24	O^+	250	4	252	21.4	6.38	-1	- .909	-3.56	-3.56	1.50 -3
25	O^+	250	4	270	21.4	6.83	-1	- .974	-3.82	-3.82	1.24 -4
26	O^+	250	4	277.	21.4	7.02	-1.	-1.	-3.92	-3.92	0.

t n at right means $\times 10^{t\,n}$

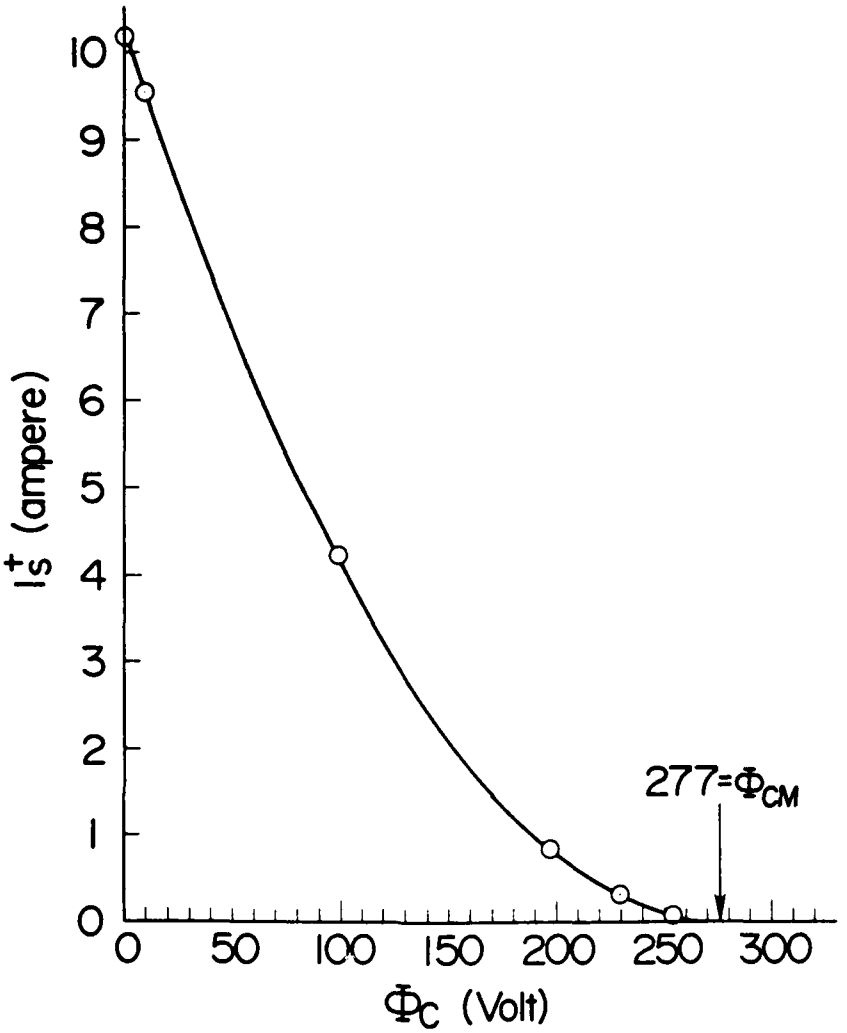

Figure 7. The O^+ Current to the Side of the Cylinder as a Function of ϕ_c for a = 250 m

$$v_T = \sqrt{\frac{kT}{2\pi m}} \quad . \tag{32}$$

So,

$$I = I_s^+ + I_e^+ + I_e^- , \tag{33}$$

and, for steady state,

$$I = 0, \tag{34}$$

where I_s^+ is given by Eqs. (28) and (29). For a = 25 or 250 m and the parameter values in Table 1, ϕ_c = -0.26 or -0.61 V, respectively, in steady state. This is determined by solving Eqs. (33) and (34) for the ϕ_c in Eq. (31). It, and thus I_s, are almost independent of the ϕ_c in c_2 in Eq. (28) for $|\phi_c| << |\phi_{cM}|$.

Now the time response resulting from capacitance is calculated. Using Eqs. (28) through (33),

$$\frac{dq}{dt} = I = C\frac{d\phi_c}{dt} = a_1(-a_2 + a_3\phi_c)^2 + a_4 - a_5 \exp(a_6\phi_c), \tag{35}$$

where q is the charge on and C the capacitance of the cylinder, the a_i's > 0 and are independent of ϕ_c and t. The value of C is obtained from Smythe's slightly modified empirical formula[18] for b = 4 and a = 250 m. The result is 61.8 nf. $\phi_{c\infty}$, the steady state value of ϕ_c at $t = \infty$, is obtained by setting Eq. (35) to 0 and solving for the ϕ_c in the exponential (as near the end of the previous paragraph). Eq. (35) could not be integrated. However, since $|\phi_c| << |\phi_{cM}|$, $a_3|\phi_c| << a_2$ (indicating that I^+ is nearly constant). So, by replacing $a_3\phi_c$ with $a_3\phi_{c\infty}$ (with very little error), Eq. (35) could be integrated, giving

$$\phi_c = \frac{1}{a_6}\ln\frac{h}{1 - (1 - h)\exp(-a_5a_6ht/C)}, \tag{36}$$

assuming $\phi_c = 0$ at t = 0, where

$$h \equiv [a_1(-a_2 + a_3\phi_{c\infty})^2 + a_4]/a_5 = \exp(a_6\phi_{c\infty}). \tag{37}$$

Figure 8 shows $\phi_c/\phi_{c\infty}$ as a function of t for $\phi_{c\infty}$ = -0.61 V and the parameter values in Table 1 with a = 250 m. This is equivalent to the potential falling exponentially from zero to $\phi_{c\infty}$ with a time constant increasing from τ_o at t = 0 to τ_∞ at $t = \infty$, where

$$\tau_o = \phi_{c\infty}\left[\frac{d\phi_c}{dt}\right]^{-1}_{t=0} = \frac{C\phi_{c\infty}}{I_{t=0}} = 0.089\,\text{ns} \tag{38}$$

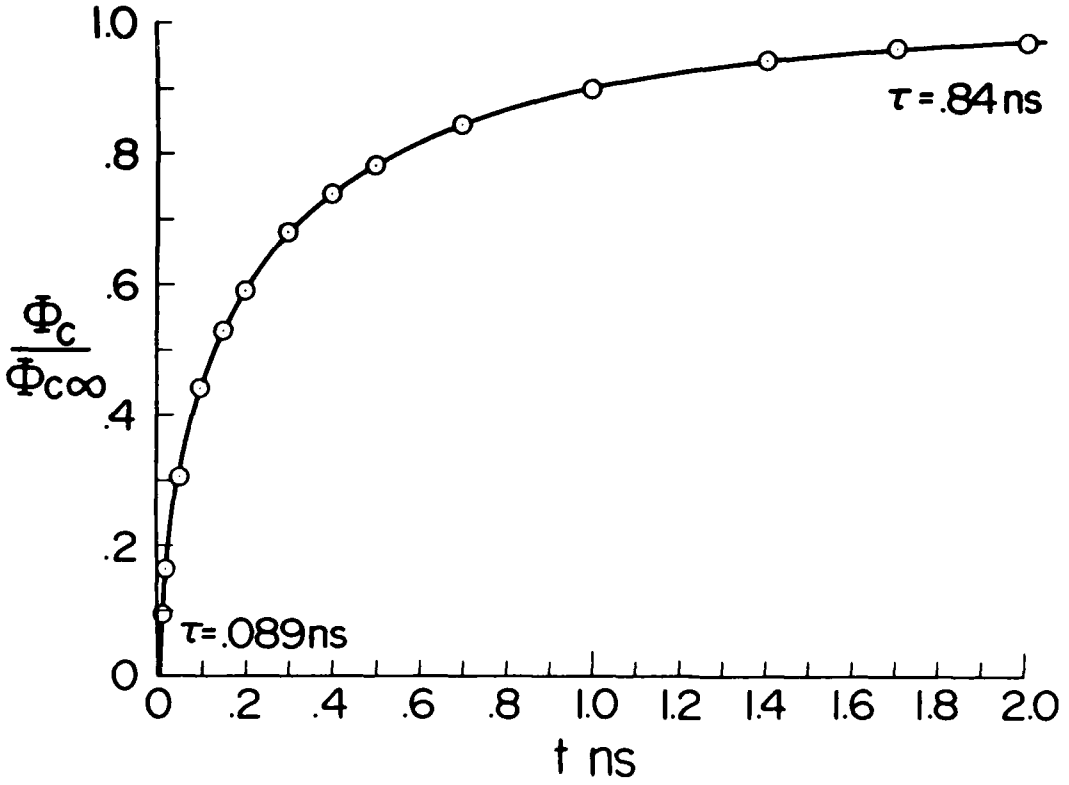

Figure 8. Normalized Cylinder Potential as a Function of Time for a = 250 m. The time constants given are those at t = 0 and ∞

and

$$\tau_\infty = \frac{C}{a_5 a_6 \exp(a_6 \phi_{c\infty})} = 0.84\,\text{ns}. \tag{39}$$

For a given value of b, $C \propto a$, but a_5, the predominant term (the electron current) in $I_{t=0}$, is proportional to a^2, so the time constant is inversely proportional to the size of the cylinder. The same calculation, but assuming that B = 0 so that $y_{\infty M} - y_{\infty m} = 2$, leads to $\phi_{c\infty} = -0.23\,\text{V}$, $\tau_0 = 0.044$ and $\tau_\infty = 0.093\,\text{ns}$. In both cases, the short time constants are the result of the small cylinder capacitance and the large electron current to the ends of the cylinder for $\phi_c > \phi_{c\infty}$. The value of b would have to be orders of magnitude larger for this current to be small or negligible compared to the electron current to the sides. Since the time constants are so small, they are rough values; full electromagnetic and mechanical equations would be required for an accurate calculation. The results show that

the charging time resulting from capacitance is small compared to particle transit times.

4. CONCLUSIONS

Simplifying assumptions lead to a relatively simple analytic theory for the steady electrical state of a body moving through a magnetoplasma. The first two orders of two-dimensional guiding center theory in the object frame are used. It leads to the potential satisfying Laplace's equation wherever all of the streamlines come from far upstream. It is applied to conditions consistent with a long, 25 m or 250 m radius, conducting, right, circular cylinder at a few hundred kilometers altitude with its axis parallel to the magnetic field and moving perpendicular to it. Hot electrons but cold ions are assumed. The potential is obtained from an empirical formula for a charged cylinder moving across a uniform magnetic field in a vacuum. Choosing $f = 1 - b/[R^2(b - 1 + R)]$ would make Eqs. (17) and (19) slightly more accurate. No charge in the plasma to balance that on the cylinder is assumed. The potential field, particle trajectories, and currents are calculated. The magnetic field decreases the ion current significantly. Because of their light mass, nearly all electrons that approach the curved surface go around the cylinder without hitting it, so the electron current to the sides is negligible. The currents to the ends of the cylinder are the same as without any magnetic field.

"Forbidden" regions next to the cylinder are found which upstream ions do not reach. The potential caused by charge density in these regions, ram and wake, and its effect on the polarization charge are neglected. If they were not and if charge balance were assumed, the forbidden region at $y > -0.5$, essentially an electron sheath, would be smaller, and the one near $y = -1$ would probably be replaced by a positive ion sheath. Since these neglected effects are important, the results may be regarded as a zeroth order approximation. The results lead to trajectories on the wake side being symmetric to those on the ram side, except that the wake side lacks those that hit the cylinder. (The charge in this region of the wake is also neglected.) Thus, there is no particle impact on the wake side and no ion focusing.

For the cylinder charged to -0.5 V, the trajectories are simple for radii greater than 47 m. For them, the ion current to the sides increases quadratically with decreasing cylinder potential. The floating potential is -0.26 or -0.61 V for the radius equal to 25 or 250 m, respectively.

The charging time constant resulting from the capacitance of the cylinder is inversely proportional to its linear dimensions. For a cylinder with a 250 m radius, simple theory results in less than a nanosecond time constant. This is neg-

ligible compared to transit times, which must therefore govern the charge-up time.

This treatment is the thick sheath approximation. The results of Smetana[19] indicate that, at least for no magnetic field, less than 10 percent error is made in the attracted species flux for $|\phi| < 4kT/|e|$. The thickness of the forbidden region at $y > -0.5$ is the order of R_g [defined in Eq. (24)]. Since a Laplacian potential is used throughout the whole plasma, the effect of Debye length is omitted.

The effect of charge in the (much thinner) forbidden regions would be largely cancelled by balancing the charge in the plasma with the charge on the cylinder. A comparison with the results of including these effects in two or more iterations would be interesting. This would indicate the accuracy of the solution here, give a better solution, and indicate how rapidly it converges to the latter. The larger cylinder treated here has a radius the same order of magnitude as the mean free path. So, either collisions should be taken into account or a smaller size should be chosen.

Treatment of other body orientations, shapes, and orbits would be of interest. Generally, this would mean attempting to extend this treatment to three dimensions. Since the velocity of a satellite at 200- or 300-km altitude is only an order of magnitude or less larger than the ion thermal motion, including the latter in the treatment would be desirable. Waves and turbulence, especially for large, irregular bodies such as the shuttle, may exist and thus also should be considered. The effect of the finite ion (but not usually electron) gyroradius must be included for bodies as small as or smaller than the shuttle. For the magnitude of cylinder charge small, the electric field vanishes along two lines on the cylinder parallel to the axis, one on the ram and one on the wake side. For the magnitude of this charge large, the electric field vanishes on a line away from the cylinder parallel to the axis at $x = 0$. Thus, the guiding center approximation breaks down in the vicinity of this (these) line(s). Calculations of trajectories that come close to this vicinity may thus be in error. For comparison, a calculation of the case treated here but with no magnetic field would be interesting.

A calculation using the POLAR code is being done for comparison. Preliminary results with an octagonal cylinder 200 m long and 50 m across at -0.26 V potential include 0.26 A ion and 0.03 A net current compared with 0.96 and 0 A, respectively, here. POLAR gives no forbidden region on the ram side of radial extent larger than ~10 m.

---

19. Smetana, F.O. (1963) On the current collected by a charged circular cylinder immersed in a two-dimensional rarefied plasma stream, in Rarefied Gas Dynamics (Vol. II), L.A. Laurmann, Ed., pp. 65-91.

References

1. Kagan, Y.M., and Perel, V.I. (1964) Probe methods in plasma research, Sov. Phys.-Usp. 81:767-793.
2. Chen, F.F. (1965) Electric probes, in Plasma Diagnostic Techniques, R.H. Huddlestone and S.L. Leonard, Eds., Academic Press, New York, 113-200.
3. Laframboise, J.G. (1966) Theory of Spherical and Cylindrical Langmuir Probes in a Collisionless, Maxwellian Plasma at Rest, U.T.I.A.S. Report 100.
4. Chung, P.M., Talbot, L., and Touryan, K.J. (1974) Electric probes in stationary flowing plasmas: Part 1. Collisionless and transitional probes, AIAA J. 12:133-154.
5. Sanmartin, J.R. (1970) Theory of a probe in a strong magnetic field, Phys. Fluids 13:103-116.
6. Rubinstein, J., and Laframboise, J.G. (1983) Aligned spheroids, finite cylinders, and disks, Phys. Fluids 26:3624-3627.
7. Call, S.M. (1969) The interaction of a satellite with the ionosphere, School Eng. Appl. Sci., Columbia U. Plasma Lab. Rept. No. 46.
8. Gurevich, A.V., Pitaevskii, L.P., and Smirnova, V.V. (1969) Ionospheric aerodynamics, Space Sci. Rev. 9:805-871 or (1970) Sov. Phys.-Usp. 99:595-616.
9. Al'pert, J.J. (1976) Wave-like phenomena in the near-earth plasma and interactions with man-made bodies, in Handbuch der Phys., Geophys. III, K. Rawer, Ed., pp. 217-349.
10. Whipple, E.C. (1981) Potentials of surfaces in space, Reprints Progr. Phys. 44:1197-1250.
11. Garrett, H.B. (1981) The charging of spacecraft surfaces, Rev. Geophys. Space Phys. 19:577-616.
12. Brundin, C.L. (1963) Effects of charged particles on the motion of an earth satellite, AIAA J. 11:2529-2538.

13. Drell, S.D., Foley, H.M., and Ruderman, M.A. (1965) Drag and propulsion of large satellites in the ionosphere; an Alfven propulsion engine in space, Phys. Rev. Lett. 14:171-175.

14. Whipple, E.C. (1965) The Equilibrium Electric Potential of a Body in the Upper Atmosphere and in Interplanetary Space. Ph.D. thesis, George Washington U., Washington, D.C.

15. Grabowski, B., and Fischer, T. (1975) Theoretical density distribution of plasma streaming around a cylinder, Planet. Space Sci. 23:287-304.

16. Brooks, W.S.C., and Koehler, J.A. (1980) The ram effect for a conducting cylinder in a drifting plasma, Can. J. Phys. 58:224-231.

17. Northrop, T.G. (1963) The Adiabatic Motion of Charged Particles, Interscience Publishers, p. 8.

18. Dubs, C.W. (1982) Potentials and Charges on Conducting Rocket Sections, AFGL-TR-82-0349, AD A130143, p. 29, Eq. (A11).

19. Smetana, F.O. (1963) On the current collected by a charged circular cylinder immersed in a two-dimensional rarefied plasma stream, in Rarefied Gas Dynamics (Vol. II), L.A. Laurmann, Ed., pp. 65-91.

END

DTIC

8-86